



Theoretical study of the mechanism and regioselectivity in the formation of pyrazolo[1,5-a]-[1,3,5]-triazines and pyrazolo[1,5-a]-[1,3,5]triazinones: a DFT study

Marwa Manachou, Christophe Morell, Henry Chermette, Salima Boughdiri

► To cite this version:

Marwa Manachou, Christophe Morell, Henry Chermette, Salima Boughdiri. Theoretical study of the mechanism and regioselectivity in the formation of pyrazolo[1,5-a]-[1,3,5]-triazines and pyrazolo[1,5-a]-[1,3,5]triazinones: a DFT study. Chemical Physics Letters, 2019, 727, pp.95-104. <10.1016/j.cplett.2019.04.054>. <hal-02108912>

HAL Id: hal-02108912

<https://hal.science/hal-02108912v1>

Submitted on 26 Nov 2020

HAL is a multi-disciplinary open access archive for the deposit and dissemination of scientific research documents, whether they are published or not. The documents may come from teaching and research institutions in France or abroad, or from public or private research centers.

L'archive ouverte pluridisciplinaire **HAL**, est destinée au dépôt et à la diffusion de documents scientifiques de niveau recherche, publiés ou non, émanant des établissements d'enseignement et de recherche français ou étrangers, des laboratoires publics ou privés.



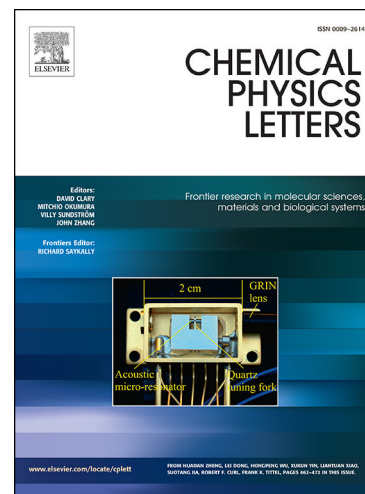
HAL Authorization

Marwa Manachou, Christophe Morell, Henry Chermette, Salima Boughdiri

To appear in: *Chemical Physics Letters*

Please cite this article as: M. Manachou, C. Morell, H. Chermette, S. Boughdiri, Theoretical study of the mechanism and regioselectivity in the formation of pyrazolo[1,5-a]- [1,3,5]-triazines and pyrazolo[1,5-a]-[1,3,5]triazinones: a DFT study, *Chemical Physics Letters* (2019), doi: <https://doi.org/10.1016/j.cplett.2019.04.054>

This is a PDF file of an unedited manuscript that has been accepted for publication. As a service to our customers we are providing this early version of the manuscript. The manuscript will undergo copyediting, typesetting, and review of the resulting proof before it is published in its final form. Please note that during the production process errors may be discovered which could affect the content, and all legal disclaimers that apply to the journal pertain.



Theoretical study of the mechanism and regioselectivity in the formation of pyrazolo[1,5-a]-[1,3,5]-triazines and pyrazolo[1,5-a]-[1,3,5]triazinones: a DFT study.

Marwa Manachou^a · Christophe Morell^b · Henry Chermette^b · Salima Boughdiri^a

a. Laboratoire de caractérisations, applications et modélisations des matériaux. Faculté des Sciences de Tunis, Université Tunis El Manar, 2092-Tunis, Tunisie

E-mail: salima.boughdiri@laposte.net

b. Institut des Sciences Analytiques, UMR 5280 CNRS/ Université Claude Bernard Lyon 1, Université de Lyon, 5 rue de la Doua, 69622 Villeurbanne Cedex, France

E-mail: henry.chermette@univ-lyon1.fr

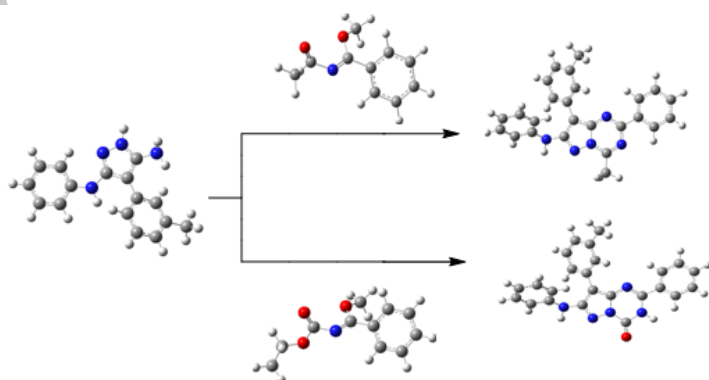
Highlights

- Geometry optimization of all reactants was carried out using DFT methods.
- Theoretical results allowed to explain the regioselectivity observed experimentally for synthesis of pyrazolo[1,5-a][1,3,5]triazine and pyrazolo[1,5-a][1,3,5] triazinones.
- Determine transition states of the different steps encountered in this reaction.
- Propose reaction mechanism by theoretical calculations.

Abstract

To shed more insight into the regioselectivities observed in the reactions between 3,5-diaminopyrazoles and N-acyl imidates or N-ethoxy imidate yielding the corresponding substituted pyrazolo[1,5-a]-[1,3,5] triazines or pyrazolo[1,5-a][1,3,5] triazinones, DFT calculations are carried out using B3LYP/6-31++G (d, p) method. The favored mechanism and the experimental regioselectivity of this reaction are rationalized by calculations of activation energy, natural atomic charge, and Fukui indexes derived from density functional theory. The present study shows that the experimental trends of the relative reactivities and regioselectivities of these reactions are correctly predicted using these computational levels.

Graphical abstract



Keywords: DFT calculation, Theoretical mechanism, Fukui function, regioselectivity, Transition state, heterocyclic system, pyrazolotriazine

1 Introduction

The pyrazolotriazine core can be found in the structure of different biologically active [1] molecules such as antifungal, antitubercular, antibacterial, antiviral anticancer and antioxidant agents... [2-5]. In particular pyrazolo[1,5-a][1,3,5]triazine, the heterocyclic system is an analogue of purine, and this scaffold has been investigated particularly in the area of nucleoside chemistry for developing biologically active agents [6]. Pyrazolo[1,5-a][1,3,5]triazine was synthesized for the first time by Checchi and Ridi, in 1957 [7]. Since that time, several approaches have been developed for the preparation of compounds with the pyrazolotriazine scaffold. The most frequently utilized approach to construct the pyrazolo[1,5-a][1,3,5]triazine heterocyclic system is the 1,3,5-triazine ring annulation method [8]. Suitable pyrazoles can be cyclized to form pyrazolo[1,5-a][1,3,5] triazines[9]. The N-acyl imidates and the N-ethoxy imidate are efficient bielectrophiles that have been used in the synthesis of many heterocyclic compounds [10]. Recently, a report [11] of an effective and versatile method for obtaining new pyrazolo [1,5-a] - [1,3,5] -triazines (P1a-d) and pyrazolo [1,5-a] [1,3,5] triazinones (P2 a-b) appeared (Table 1). It is obtained by the interaction of N-acyl imidates (R2 a, b) or N-ethoxy imidate (R2) with 3,5-diaminopyrazoles (R1 a-d) under the influence of acetic acid (Scheme 1) . It should be also mentioned that the regiochemistry of the ring closure was not always unambiguous; the structure assignments were often uncertain and therefore require further verification. Hence the purpose of this study is to better understand the reactions opposing N-acyl imidates or N-ethoxy imidate to 3,5-diaminopyrazoles to obtain novel pyrazolo[1,5-a]-[1,3,5]-triazines or pyrazolo [1,5-a] [1,3,5] triazinones , by clarifying the nature of the transition states, the origin of the regioselectivity and the effects of the substituent.

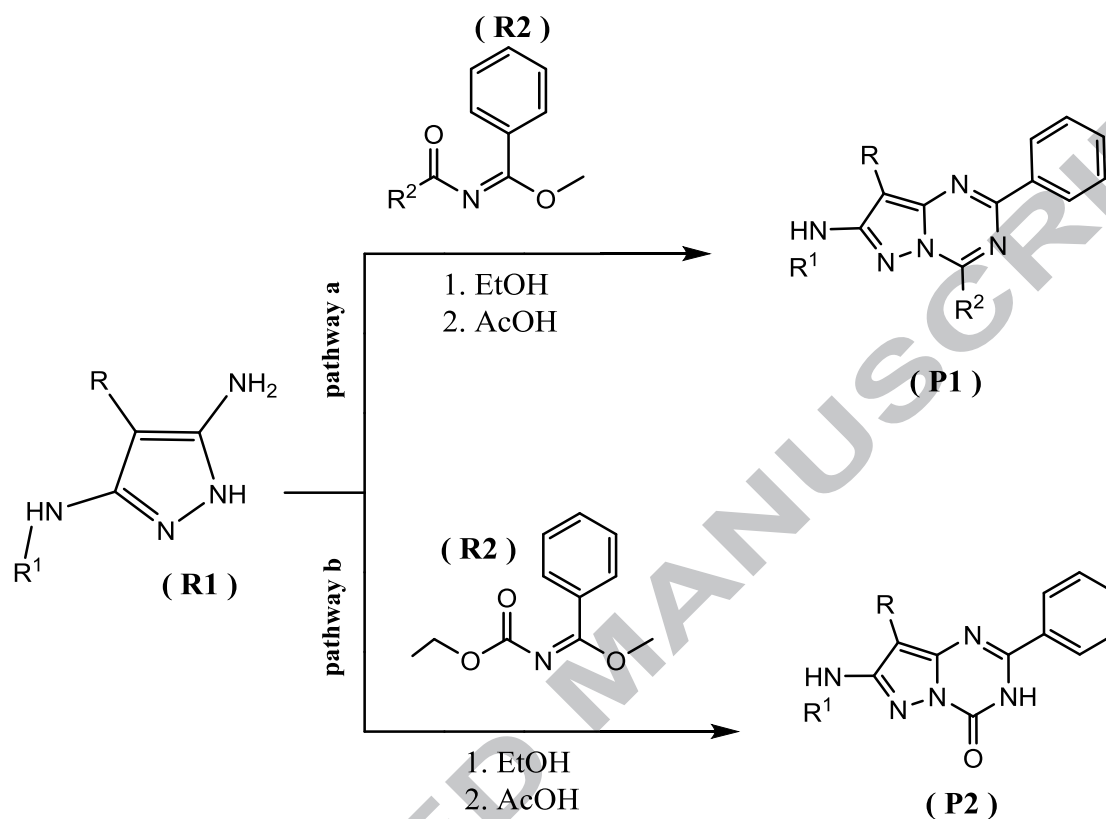
Besides, in order to predict the products of this reaction we have attempted to rationalize the mechanisms thanks to conceptual DFT descriptors such as chemical potential, hardness, Fukui functions and electrophilicity index [12-17].

In a first section of this paper, computational details are given and the reactivity indexes used in the present work are introduced. In Sect. 2, a detailed discussion of the outcome of the reaction is provided. The paper ends with some concluding remarks.

Table 1 Series (R, R1, R2) and the yields of synthesized compounds

Product	R	R ¹	R ²	Yield, %
P1 a	m-CH ₃ -C ₆ H ₄	Ph	CH ₃	64
P1 b	Ph	c-C ₆ H ₁₁	CH ₃	76
P1 c	Ph	Ph-CH ₂ -	Ph-CH ₂ -	77
P1 d	Ph	Ph	Ph-CH ₂ -	81
P2 a	m-CH ₃ -C ₆ H ₄	Ph	O-C ₂ H ₆	65
P2 b	Ph	c-C ₆ H ₁₁	O-C ₂ H ₆	67

Scheme 1: Pathway (a) Synthesis of pyrazolo[1,5-a]-[1,3,5] triazines pathway (b) Synthesis of pyrazolo[1,5-a][1,3,5] triazinones.



2 Computational details:

All calculations were done with the GAUSSIAN 09 [18] package of quantum chemistry programs. Geometry optimization of all reactants and products was carried out using DFT methods at the B3LYP/6-31++G(d,p) level of theory [19, 20], in gas phase, ethanol and toluene. Energies of all structure are calculated using B3LYP with Grimme D3 corrections, updated to include dispersion correlation [21] parameterized by Becke-Johnson (D3BJ) [22] and 6-31++G(d,p) basis set [23-25], on the obtained structures in gas phase, ethanol and toluene. The effect of solvent were taken into account using the conductor like polarizable continuum (CPCM) model in its standard implementation in the Gaussian code [26]. The chosen compounds are those experimentally studied and are gathered in Table 1. The transition states (TSs) geometries for these reactions have been calculated at the same level of theory. All the structures were characterized by vibrational analysis in the harmonic approximation, with no imaginary frequency for optimizations of all reactant and product structures and a single one for transition states [27-28]. The conceptual DFT descriptors have been computed using the so-called frozen orbitals approximation and the Koopmans' theorem [29]. In other words, indexes have been calculated using only frontier orbital densities and frontier energies and condensed indices through atomic populations. The electronic structures of stationary points were analyzed by the natural bond orbital (NBO) method [30-31].

2.1 Global reactivity indexes

In order to describe the reactivity and the stability of a system, popular qualitative chemical concepts derived from conceptual DFT [32-33] such as the chemical potential μ [34] (Eqn. 1), hardness η (Eqn. 2) and even the electrophilicity index ω (Eqn. 5), have been calculated [35-36].

$$\mu = \left(\frac{\partial E}{\partial N} \right)_{v(r)} \quad (1)$$

$$\eta = \left(\frac{\partial^2 E}{\partial N^2} \right)_{v(r)} \quad (2)$$

$E_{v(r)}$ is the total energy of the system,

N : represents its number of electrons.

$v(r)$: indicates that the derivatives are taken at constant external potential [37].

These indexes are often approximated through frontier orbital eigenvalues, leading to:

$$\mu \cong (E_{\text{HOMO}} + E_{\text{LUMO}})/2 \quad (3)$$

$$\eta \cong (E_{\text{LUMO}} - E_{\text{HOMO}}) \quad (4)$$

Where E_{HOMO} and E_{LUMO} are the energies of the highest occupied and lowest unoccupied molecular orbitals (HOMO and LUMO), respectively [38].

The electrophilicity index as defined by Parr et al. [39] is the stabilizing energy a system gets when it acquires enough electrons to be saturated. It is therefore a measure of its ability to accommodate extra electrons.

$$\omega = \mu^2/2\eta \quad (5)$$

2.2 Local reactivity indexes

To describe site selectivity or reactivity of an atom k in a molecule, the condensed Fukui functions f_k^+ and f_k^- [40-41] have been considered. This latter are calculated from electronic population analysis.

$$f_k^+ = [q_k(N+1) - q_k(N)] \quad (6)$$

for nucleophilic attack.

$$f_k^- = [q_k(N) - q_k(N-1)] \quad (7)$$

for electrophilic attack.

In Eqs. 6 and 7, k is the numbering of the atomic site, $q_k(N)$, $q_k(N-1)$ and $q_k(N+1)$ stand for the atomic charges on site k in neutral, cationic and anionic systems, respectively. [42] Finally, the dual descriptor (DD) $\Delta f(r)$, introduced by Morell [43-44], which characterizes how the absolute hardness changes when the external potential changes, is obtained, in its condensed form, by:

$$\Delta f_k(r) = f_k^+ - f_k^- \quad (8)$$

3 Results and discussion

3.1 Analysis based on energetic aspects

3.1.1 Reaction Energies.

In this main section, we investigate the performance of density functional with and without dispersion correction. Deviations energies between the values computed with and without inclusion of dispersion corrections are given in Fig.1. The B3LYP-D3(BJ) functional leads to significantly larger energies with respect to B3LYP. As expected, the systems, particularly the products, are strongly stabilized by intramolecular dispersion effects. This energy stabilization lies within the 30-35 kcal mol⁻¹ range. Nevertheless, this extra-stabilization lies in the same range for all compounds, and the reaction energies and barrier energies remain similar. In the rest of the paper, all the reported energies take the dispersion corrections into account. The corresponding energies calculated at the B3LYP level are given in the Supplementary Data section.

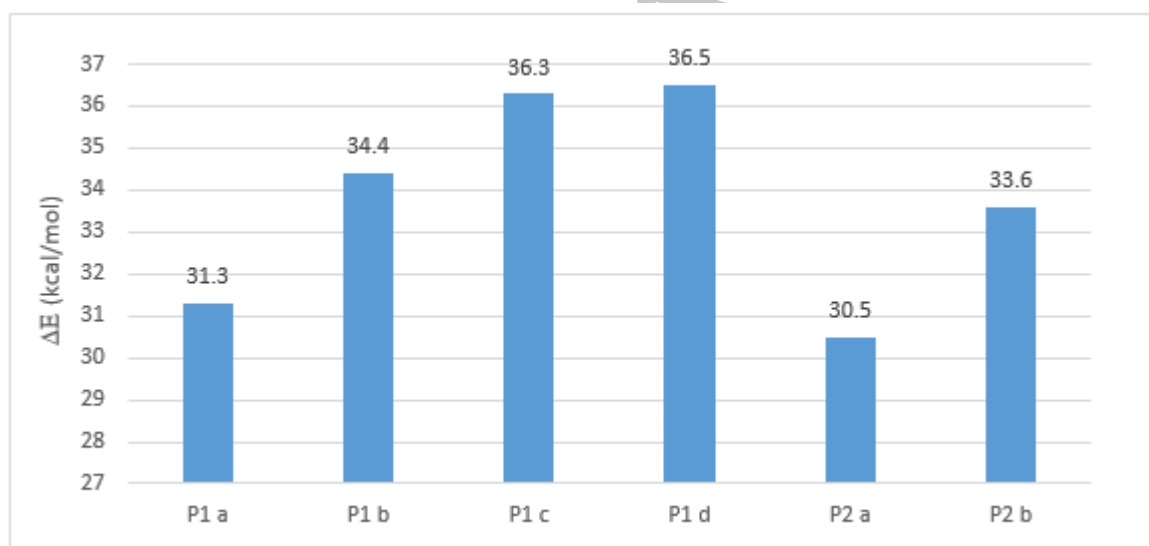


Fig. 1. Deviations energies between the values computed at the DFT B3LYP /6-31++G(d,p) level of theory with and without dispersion correlation (D3BJ) for products P1a-d and P2a-b in gas phase: $\Delta E = E(\text{B3LYP}) - E(\text{B3LYP-D3(BJ)})$

3.1.2 Thermochemical parameters

In order to observe possible effects of the substituents and the solvents, we performed quantum mechanics calculations, for different substituents (P1a—P1d) and (P2a, P2b), in gas phase, in ethanol and toluene using CPCM model to obtain thermodynamic parameters such as Gibbs free energy ΔG and enthalpy ΔH for all products. Table 2 lists the energetics (ΔG° and ΔH° at $T = 25^\circ\text{C}$ and $P = P^\circ = 1\text{ bar}$)

Table 2 Thermodynamic data (in kcal mol⁻¹), in Gas phase, Ethanol and Toluene, for the pyrazolo[1,5-a]-[1,3,5]-triazines(P1) and pyrazolo [1,5-a] [1,3,5] triazinones (P2)

<i>Solvent</i>	Gas phase		Ethanol		Toluene	
<i>Products</i>	ΔG°	ΔH°	ΔG°	ΔH°	ΔG°	ΔH°
<i>P1a</i>	-20.38	-14.28	-17.96	-11.69	-19.17	-13.17
<i>P1b</i>	-22.95	-15.95	-20.33	-13.42	-21.59	-14.86
<i>P1c</i>	-26.00	-18.45	-22.82	-15.56	-23.66	-17.24
<i>P1d</i>	-20.31	-13.75	-17.71	-10.75	-18.43	-12.45
<i>P2a</i>	-17.84	-10.21	-18.92	-12.38	-23.57	-16.10
<i>P2b</i>	-19.83	-11.72	-22.16	-13.41	-25.83	-17.69

As it can be seen from Table 2, the reaction is exothermic. The order of stability of pyrazolo[1,5-a]-[1,3,5]-triazines or pyrazolo [1,5-a] [1,3,5] triazinones in gas phase is influenced by the nature of the substituent. Therefore, the compound P1c is the most stable one. The substitution of an attractor group (phenyl ring) improves the stability of the product ($\Delta G^\circ = -26$ kcal/mol). Using ethanol or toluene as solvent, we have noticed that the compound P1c remains the most stable one, even slightly more stable in toluene ($\Delta G^\circ = -23.7$ kcal/mol) than in ethanol ($\Delta G^\circ = -22.8$ kcal/mol). However the solvation affects the order of stability, the product P2b being the most stable in toluene ($\Delta G^\circ = -25.8$ kcal/mol). Consequently, the order of stability is affected by both of the nature of the substituent and of the solvent. Based on the previous results, it is not possible to conclude that the compound P1c is the most stable one. These results are similar to those obtained experimentally.

3.2 Acetic acid effect

The mechanism of the reaction is likely to proceed via the protonation of N-acyl imidates or the N-ethoxy imidate (R2). In fact the reaction of diaminopyrazole with appropriate biselectrophiles to give pyrazolo[1,5-a]-[1,3,5]-triazines or pyrazolo[1,5-a]-[1,3,5] triazinones (only) occurred experimentally in the presence of acetic acid (AcOH). Based on this, and as discussed hereafter, protonation of R2 lowered the LUMO–HOMO gap and makes the reaction easier. Indeed, as presented in Fig. 2 the two possible relative energy interactions ΔE_1 and ΔE_2 can be defined as:

$$\Delta E_1 = \text{LUMO}_{R2} - \text{HOMO}_{R1} \text{ and } \Delta E_2 = \text{LUMO}_{R1} - \text{HOMO}_{R2}$$

The frontier molecular orbital (FMO) analysis for this reaction shows that the main interactions occur between the HOMO (R1) and the LUMO (R2), and the calculated ΔE_{L-H} for biselectrophilic ($\Delta E_1 = -1.58$ eV) in presence of acetic acid is lower than that without catalyst ($\Delta E_1 = 3.61$ eV).

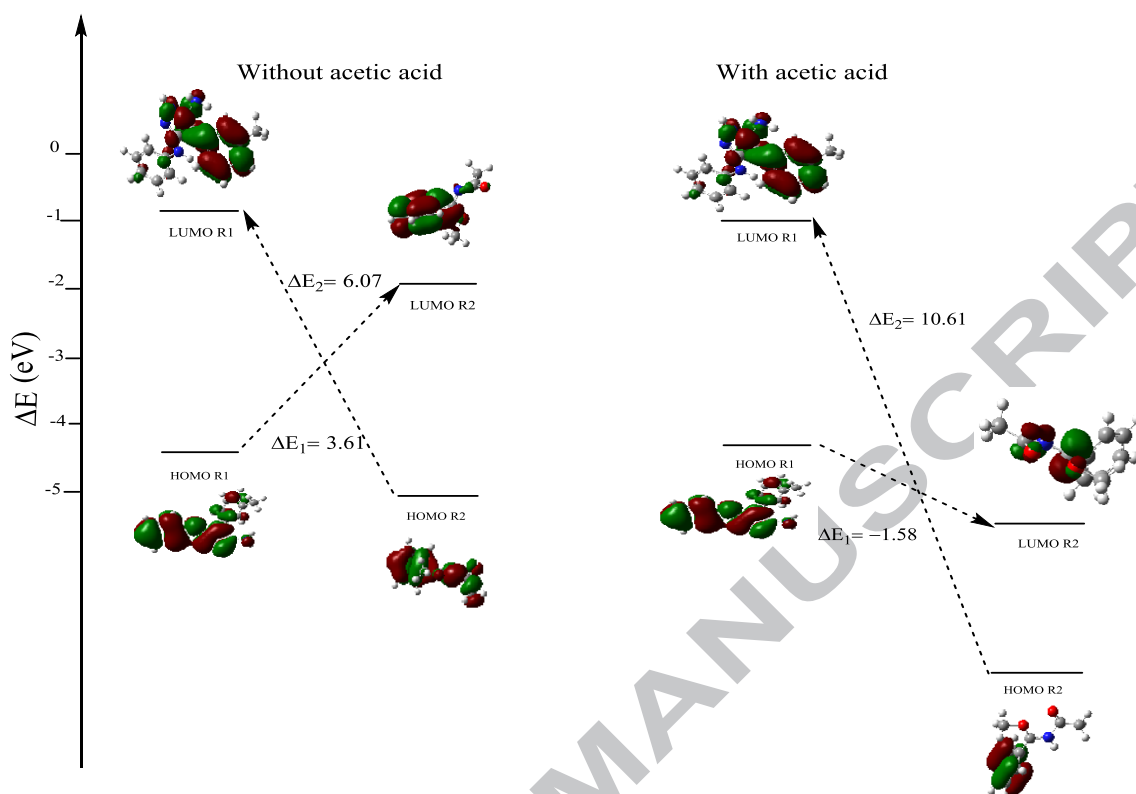


Fig. 2. Effect of AcOH on frontier molecular orbital diagram of the reactions between the diaminopyrazole and opposing N-acyl imidates (P1 a). Energies in eV

Table 3 Global reactivity descriptors (μ , η , ω) in eV for 3,5-diaminopyrazoles and N-acyl imidates in gas phase (Effect of AcOH)

Reactants	R1	R2	
		without AcOH	with AcOH
μ (eV)	-2.957	-4.188	-9.055
η (eV)	2.181	2.662	2.335
ω (eV)	2.005	3.295	17.559

In addition to the FMO theory, global descriptors have been used to study the chemical reactivity of the reactants. The global electrophilicity index, hardness and chemical potential are calculated (Table 3), it can be noticed that the presence of AcOH improves the charge transfer between R1 and R2 ($\mu = -4.188$ eV to -9.055 eV) and the electrophile character of the reagent R2 ($\omega = 3.295$ eV to 17.559 eV).

In order to determine the influence of on the protonation of the site of attack we have calculated local reactivity descriptor. It can be noted from Table 4 and 5 that the protonation of R2 can orientate the site of attack towards the isomer obtained experimentally.

Table 4 Selected Natural Bond Orbital (NBO) charge q and local reactivity descriptor f_k^- for the series of the (R1) 3,5-diaminopyrazoles in gas phase

R ₁	NH_2	R1	f_k^-	qN
----------------	---------------	----	---------	----

N_1	0.054	-0.381
N_2	0.076	-0.411
N_3	0.020	-0.863
N_4	0.177	-0.610

Table 5 Selected Natural Bond Orbital (NBO) charge q and local reactivity descriptor f_k^+ for the series of N-acyl imidates in gas phase (Acetic acid effect)

index	Without AcOH		With AcOH	
	f_k^+	qN	f_k^+	qN
C_1	0.091	600.611	0.099	0.755
C_2	0.004	0.695	0.190	0.712

It can be concluded from the values of qN and f_k^+ that the intervention of acetic acid on R2 changes the site of attack to obtain the experimental product. (Fig. 3)

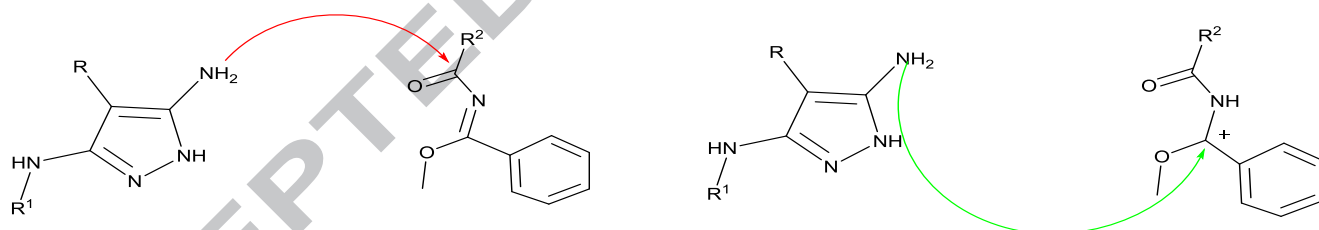
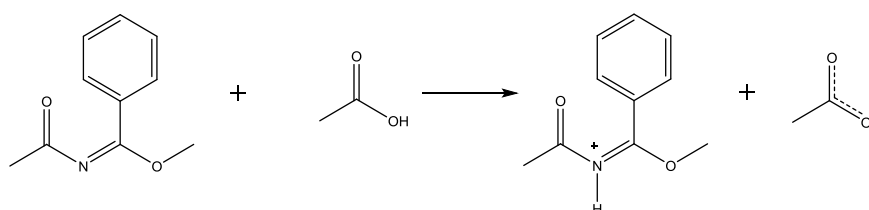


Fig. 3. Effect of AcOH on the selectivity of the diaminopyrazole on N-acyl imidates

It turns out from the present study that diaminopyrazole attacks the N-acyl imidates or the N-ethoxy imidate to obtain pyrazolo[1,5-a]-[1,3,5]-triazines or pyrazolo [1,5-a] [1,3,5] triazinones is only possible through a proton exchange between N-acyl imidates or the N-ethoxy imidate and acetic acid. (Scheme 2)

Scheme 2 Mechanism of the protonation of N-acyl imidates by acetic acid



3.3 Reaction between 3,5-diaminopyrazoles and N-acyl imidates or N-ethoxy imide

3.3.1 Chemical Reactivity

It was found experimentally that the reaction between 3,5-diaminopyrazoles and N-acyl imidates or N-ethoxy imide under the influence of acetic acid give pyrazolo[1,5-a]-[1,3,5]-triazines or pyrazolo [1,5-a] [1,3,5] triazinones, respectively. In order to study the regioselectivity observed experimentally, the frontier molecular orbitals of the 3,5-diaminopyrazoles and N-acyl imidates and N-ethoxy imide were calculated. The (LUMO) of N-acyl imidates (-6.720 eV) or N-ethoxy imide (-6.554 eV) have the smallest energy. The calculated ΔE_1 is smaller than the ΔE_2 , thus the main interactions occur between the HOMO (R1) and the LUMO (R2), located approximately at -5.13 eV and -6.72 eV (Table 5).

Table 6 Frontier orbital energy HOMO, LUMO (eV), the energy differences ΔE and the global reactivity descriptors (μ , η , S , ω) for 3,5-diaminopyrazoles and N-acyl imidates for P1 or N-ethoxy imidate for P2 in gas phase

Reaction	P1 a		P1 b		P1 c		P1 d		P2 a		P2 b	
Reagent	R1	R2	R1	R2	R1	R2	R1	R2	R1	R2	R1	R2
HOMO(eV)	-5.138	-11.391	-5.325	-11.391	-5.426	-10.165	-5.174	-10.165	-5.138	-11.307	-5.325	-11.307
LUMO(eV)	-0.776	-6.720	-0.569	-6.720	-0.609	-6.521	-0.794	-6.521	-0.776	-6.554	-0.569	-6.554
$\Delta E1$	-1.581		-1.394		-1.094		-1.347		-1.419		-1.228	
$\Delta E2$	10.614		10.821		9.555		9.370		10.525		10.737	
μ (eV)	-2.957	-9.055	-2.947	-9.055	-3.018	-8.343	-2.984	-8.343	-2.957	-8.931	-2.947	-8.931
η (eV)	2.181	2.335	2.378	2.335	2.408	1.821	2.189	1.821	2.181	2.376	2.378	2.376
ω (eV)	2.005	17.559	1.827	17.559	1.891	19.107	2.034	19.107	2.005	16.783	1.827	16.783
S (eV ⁻¹)	0.229	0.214	0.210	0.214	0.207	0.274	0.228	0.274	0.229	0.210	0.210	0.210

Table 7 Frontier orbital energy HOMO, LUMO (eV), the energy differences ΔE and the global reactivity descriptors (μ , η , S , ω) for 3,5-diaminopyrazoles and N-acyl imidates for P1 or N-ethoxy imidate for P2 in Ethanol

Reaction	P1 a		P1 b		P1 c		P1 d		P2 a		P2 b	
Reactant	R1	R2	R1	R2	R1	R2	R1	R2	R1	R2	R1	R2
HOMO(eV)	-5.385	-8.003	-5.537	-8.003	-5.644	-7.370	-5.398	-7.370	-5.385	-8.011	-5.537	-8.011
LUMO(eV)	-0.705	-3.308	-0.650	-3.308	-0.672	-3.373	-0.742	-3.373	-0.705	-3.246	-0.650	-3.246
$\Delta E1$	-2.076		-2.228		-2.271		-2.025		-2.138		-2.290	

$\Delta E2$	7.298		7.352		6.697		6.627		7.305		7.360	
μ (eV)	-3.045	-5.656	-3.093	-5.656	-3.158	-5.371	-3.070	-5.371	-3.045	-5.629	-3.093	-5.629
η (eV)	2.340	2.347	2.443	2.347	2.486	1.998	2.328	1.998	2.340	2.382	2.443	2.382
ω (eV)	1.981	6.814	1.958	6.814	2.006	7.219	2.024	7.219	1.981	6.650	1.958	6.650
S (eV ¹)	0.213	0.213	0.204	0.213	0.201	0.250	0.214	0.250	0.213	0.209	0.204	0.209

Table 8 Frontier orbital energy HOMO, LUMO (eV), the energy differences ΔE and the global reactivity descriptors (μ , η , S , ω) for 3,5-diaminopyrazoles and N-acyl imidates for P1 or N-ethoxy imidate for P2 in Toluene

Reaction	P1 a		P1 b		P1 c		P1 d		P2 a		P2 b	
Reactant	R1	R2	R1	R2	R1	R2	R1	R2	R1	R2	R1	R2
HOMO(eV)	-5.266	-9.364	-5.429	-9.364	-5.530	-8.481	-5.290	-8.481	-5.266	-9.340	-5.407	-9.340
LUMO(eV)	-0.734	-4.671	-0.606	-4.671	-0.630	-4.643	-0.756	-4.643	-0.734	-4.585	-0.606	-4.585
$\Delta E1$	-0.595		-0.758		-0.887		-0.647		-0.679		-0.822	
$\Delta E2$	8.630		8.758		7.851		7.725		8.595		8.733	
μ (eV)	-3.000	-7.018	-3.017	-7.018	-3.080	-6.562	-3.023	-6.562	-3.000	-6.962	-3.017	-6.962
η (eV)	2.266	2.346	2.411	2.346	2.449	1.919	2.267	1.919	2.266	2.377	2.411	2.377
ω (eV)	1.986	10.494	1.888	10.494	1.936	11.218	2.016	11.218	1.986	10.195	1.888	10.195
S (eV ¹)	0.220	0.213	0.207	0.213	0.204	0.260	0.220	0.260	0.220	0.210	0.207	0.210

Moreover global descriptors have been used to study the chemical reactivity of the reactants, the global electrophilicity index, hardness and softness..., have been calculated in ethanol, toluene and in gas phase to study the influence of the polarity of solvent on the reactivity of different reactants. The effect of solvent has been investigated using CPCM model. The results summarized in (Tables 6, 7 and 8) show that the electronic chemical potential of R1 (-2.95 eV) is higher than that of R2 (-9.05 eV), which indicates that the electron transfer will take place from R1 to R2. In addition, the electrophilicity of R1 ($\omega = 2.00$ eV) is lower than R2 ($\omega = 17.55$ eV) and therefore, 3,5-diaminopyrazoles (R1) behaves like a nucleophile and N-acyl imidates or N-ethoxy imidate (R2) behaves like an electrophile. All the other descriptors as global hardness and global softness converge to the same results.

The substitution of an attractor group (phenyl ring) on the reagents improves their electrophilic and nucleophilic character and consequently the yield of the reaction (experimental yields are 77 and 81%). We can note also that the electrophilicity of the reactant R2 decreases with the substituent ethoxy group. Indeed, the ω value is a little different, amounting 19.10 eV with phenyl group, to be compared to 17.55 eV with ethoxy group.

Whereas the experiments were performed in ethanol, the results in Tables 7 and 8 let conclude that the reagents are more reactive in toluene than in ethanol: the global electrophile index of R2 in ethanol ($\omega = 6.81$ eV) is lower than that of R2 in toluene ($\omega = 10.49$ eV). Therefore when the polarity of the solvent decreases, the reaction becomes favored.

3.3.2 Prediction of the regioselectivity

Chemical reactions are either controlled by charge or by frontier densities. In this context, each reactant (R1 and R2) has been characterized through conceptual DFT indices supposed to describe both effects. Then, the charge and/or orbital control of the reaction is discussed in ethanol, toluene and in gas phase.

It is plain to see from the results displayed in Tables 9, 10 and 11, that the N₄ of 3,5-diaminopyrazoles is the most nucleophilic center. It exhibits the highest value of the local Fukui index ($f_k^- = 0.177$) in the nucleophilic compound. The most electrophilic center can be characterized by the highest value of local Fukui index ($f_k^+ = 0.190$). In the electrophilic compound it is C₂ of N-acyl amides, but for N-ethoxy imidate the Fukui indices are all negative (Table 11). The theoretical results from local reactivity indices f_k^- and f_k^+ does not lead us to the experimental products; therefore the reaction might not be under orbital control. The process is very likely to be under charge control.

Table 9 Selected Natural Bond Orbital (NBO) charge q and local reactivity descriptor f_k^- for the series of the R1 3,5-diaminopyrazoles in gas phase and in different solvents

Reaction	a		b		C		d	
	Gas phase							
R1	f_k^-	qN	f_k^-	qN	f_k^-	qN	f_k^-	qN
N ₁	0.054	-0.381	0.064	-0.392	0.060	-0.396	0.056	-0.380
N ₂	0.076	-0.411	-0.102	-0.418	0.099	-0.417	0.077	-0.411

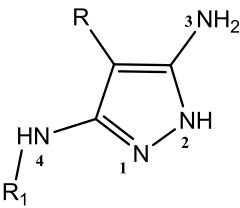
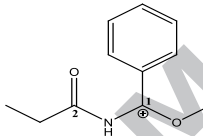
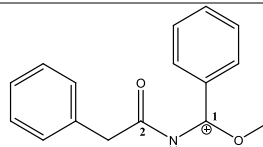
	N ₃	0.020	-0.863	-0.026	-0.864	0.024	-0.863	0.021	-0.863
	N ₄	0.177	-0.610	-0.226	-0.662	0.209	-0.660	0.179	-0.610
	Ethanol								
	N ₁	0.071	-0.416	0.061	-0.429	0.076	-0.421	0.074	-0.415
	N ₂	0.083	-0.410	-0.110	-0.417	0.086	-0.413	0.084	-0.410
	N ₃	0.016	-0.866	-0.021	-0.868	0.018	-0.868	0.017	-0.866
	N ₄	0.196	-0.614	-0.216	-0.671	0.254	-0.672	0.196	-0.613
	Toluene								
	N ₁	0.062	-0.400	0.063	-0.412	0.056	-0.41	0.064	-0.399
	N ₂	0.080	-0.410	-0.108	-0.417	0.104	-0.414	0.080	-0.410
	N ₃	0.018	-0.865	-0.025	-0.867	0.026	-0.866	0.019	-0.865
	N ₄	0.187	-0.612	-0.223	-0.667	0.208	-0.666	0.189	-0.612

Table 10 Selected Natural Bond Orbital (NBO) charge q and local reactivity descriptor f_k^+ for the series of R2 N-acyl imidates in gas phase and in different solvents

Reaction				
	Gas phase			
Index	f_k^+	qN	f_k^+	qN
C_1	0.099	0.755	0.092	0.754
C_2	0.190	0.712	0.188	0.719
	Ethanol			
C_1	0.246	0.773	0.228	0.774
C_2	0.075	0.730	0.075	0.739
	Toluene			
C_1	0.236	0.764	0.234	0.765
C_2	0.066	0.722	0.069	0.730

The study of net partial charges on atomic centers reflects the magnitude of the electrostatic force. In this paper, the net charges have been computed through the Natural Bond Orbital (NBO) scheme. The calculated charges are reported in Tables 9, 10 and 11. For the series of the 3,5-diaminopyrazoles, the lowest negative natural charge belongs to the nitrogen N₃ as nucleophilic centers with a partial natural charge around -0.863 e. One can notice that this charge is slightly higher (more negative) than -0.868e next to phenyl ring substituents and in a polar solvent like ethanol. This little difference cannot be considered as significant for selectivity.

For the electrophile, it is interesting to note that C₁ and C₂ exhibit fairly similar natural charges. For the electrophilic compounds N-acyl imidates (Table 10), the highest positive natural charge belongs to the carbon C₁ as an electrophilic center ($q(C_1) = 0.755e$). It is interesting to note that the natural charge of carbon C₂ is equal to 0.712e, a value close to

$q(C_1)$, therefore the presence of another isomer is possible, and we can also notice that the nature of the solvent as well as the nature of the substituents have not noteworthy effects on the selectivity. Consequently, the reactivity order should favor the addition of NH_2 of the pyrazole on the C_1 of the protonated N-acyl imidates (Fig. 4). This is in agreement with the experimental product therefore the reaction is under charge control.

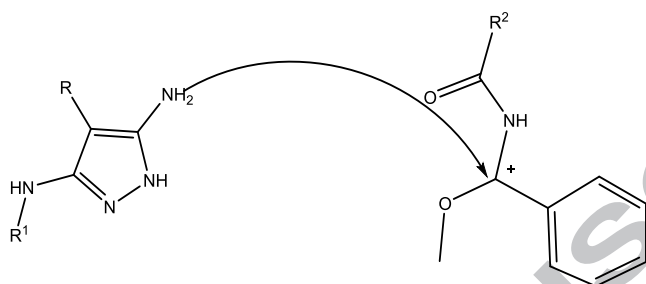
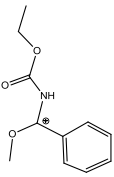


Fig. 4. Schematic representation of the first attack of the protonated N-acyl and diaminopyrazole imidates.

Table 11 Selected Natural Bond Orbital (NBO) charge q and local reactivity descriptor f_k^+ for the series of the protonated N-ethoxy imidate in gas phase and in different solvents

	Gas		Ethanol		Toluene	
	index	f_k^+	qN	f_k^+	qN	qN
	C_1	-0.229	0.750	-0.246	0.769	0.760
	C_2	-0.024	0.947	-0.040	0.967	0.958

For the N-ethoxy imidate (Table 11), the highest positive natural charge belongs to the carbon C_2 as an electrophilic center ($q(C_2) = 0.947e$) which gives the isomer of the experimental product. We note that the natural charge of carbon C_1 is equal to $0.750e$, a value near to $q(C_2)$, therefore the presence of two isomers is possible. Consequently, the reactivity order for the synthesis pyrazolo[1,5-a][1,3,5] triazinones should favor the addition of NH_2 of the pyrazole on the C_2 or C_1 of the N-ethoxy imidate (Fig. 5).

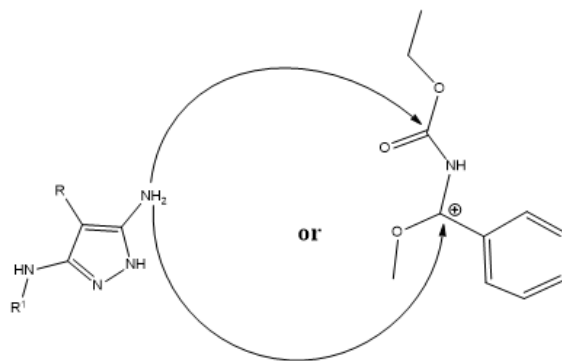


Fig. 5. Schematic representation of the first attack of the protonated N-ethoxy imidate and diaminopyrazole .

In this situation, it is necessary to examine the charge transfer to the transition state in order to favor one attack over another and settle between the two isomers.

3.4 Proposed mechanism

The previous discussion leads to believe that the reaction is under charge control. Indeed, the experimentally obtained product corresponds to the one characterized by the net partial charges on atomic centers. In the present work, the TSs are characterized through vibrational analysis. Each TS is characterized by a single imaginary frequency.

3.4.1 Reaction between 3,5-diaminopyrazoles and N-acyl imidates

Table 12 lists the activation energies associated to the transition states of the different steps encountered in the mechanism for synthesis of pyrazolo[1,5-a][1,3,5]triazine in gas phase. The energetic diagram established are shown in Fig.6

Table 12 Activation energies in (kcal/mol) for different step of the reaction between 3,5 diaminopyrazoles and N-acyl imidates to give P1(a-d), in gas phase, calculated at the DFT B3LYP-GD3(BJ)/631++(d,p) level (reference energy is the energy of the reactants)

TS	E _{a1}	E _{a2}	E _{a3}	E _{a4}	E _{a5}
PI-a	17.3	35.3	9.3	31.3	36.4
PI-b	16.5	37.6	1.47	30.5	32.5
PI-c	14.8	35.6	11.1	24.5	34.3
PI-d	18.9	33.9	17.0	28.9	37.6

An analysis of stationary points found along the reaction process indicates that this reaction occurs along a mechanism in several steps. The products P1 are formed after five transition states (TS1, TS2, TS3, TS4 and TS5). The first step of the proposed mechanism (Scheme 3) , after the protonation of N-acyl imidates, is the binding of the electrophilic center C₁ to the nucleophile center N₃. TS1 has been identified and characterized by a single imaginary frequency. Its geometry is represented in Fig. 6. The bond length C1–N3 (1.510 Å) and the computed activation energy E_{a1} amounts 17.3 kcal/mol, a value sufficiently low to believe that this stage processes smoothly.

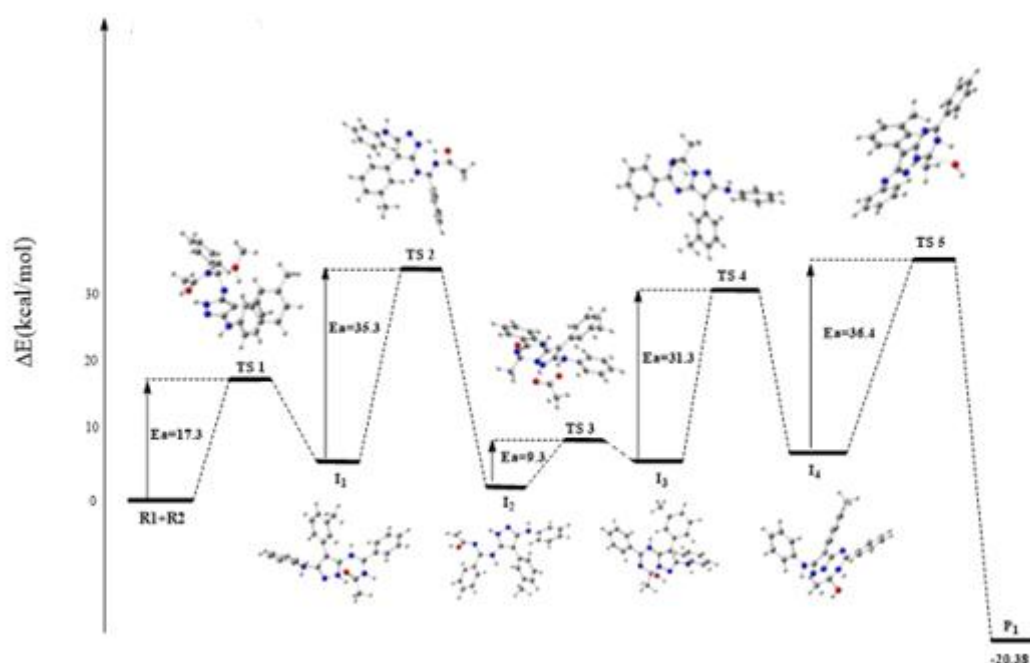
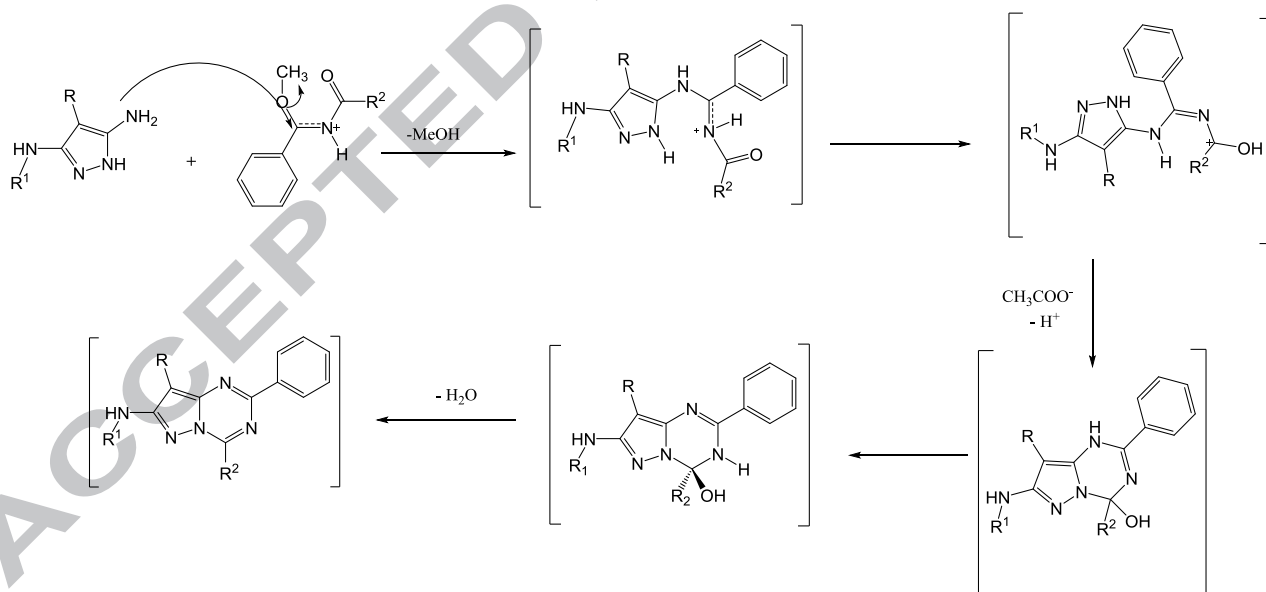


Fig. 6. Energy diagram of the reaction of 3,5-diaminopyrazoles with N-acyl imidates (P1a)

Scheme 3 Proposed mechanism for synthesis of pyrazolo[1,5-a][1,3,5]triazine



We also noticed that adding a dispersion-correction lowers the barriers such that B3LYP-D3(BJ) reduces them by about 2-8 kcal/mol. (Fig.7)

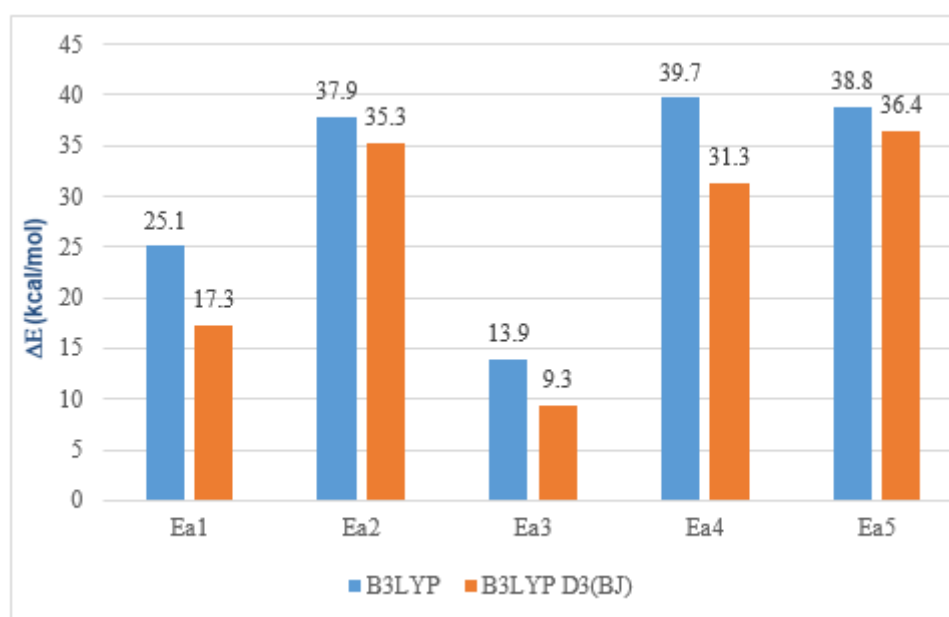


Fig.7. Activation energies ΔE in (kcal mol^{-1}) computed at the DFT B3LYP /6-31++G(d,p) level of theory with and without dispersion correlation (D3BJ). (P1a)

3.4.2 Reaction between 3,5-diaminopyrazoles and N-ethoxy imidate

As shown in Fig.8 transition state leading to the intermediates I_1 and I_2 associated of the two competing reactive attack of exocyclic nitrogen at pyrazole NH_2 on C_1 or C_2 are optimized. We can notice that the calculated activation electronic energy E_{a2} amounts to 33.7 kcal/mol. This value is higher than ($E_{a1} = 21.6 \text{ kcal/mol}$), so the I_2 formation process is more difficult and I_1 can be considered as a kinetically favored intermediate and more stable.

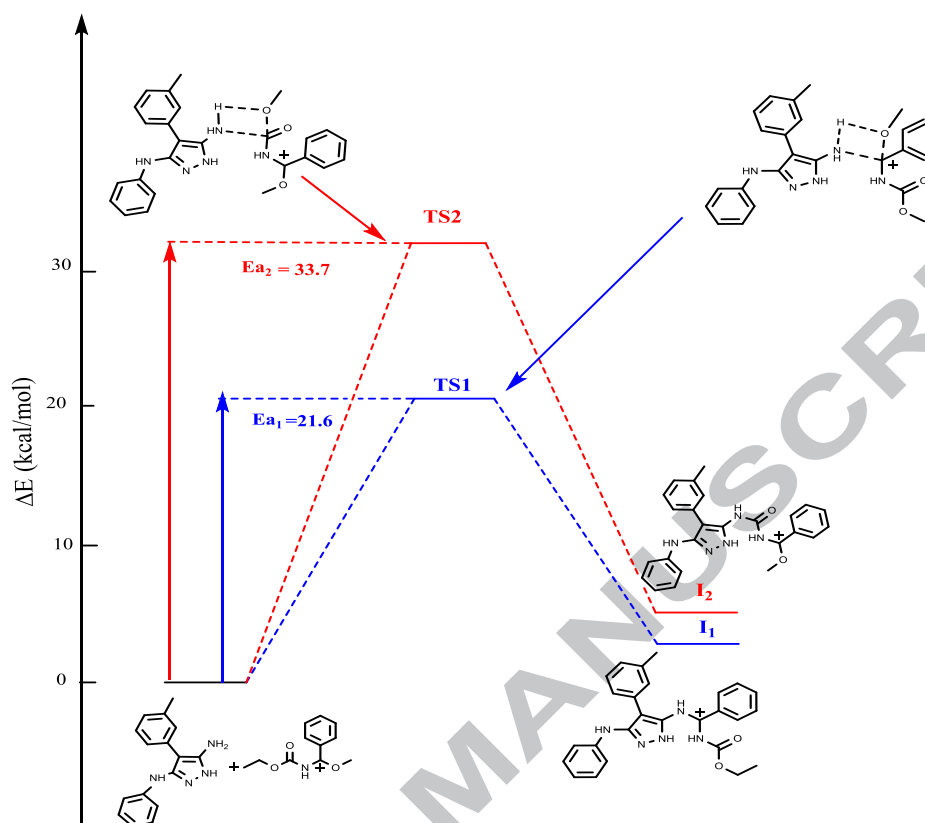


Fig. 8. Energy diagram of the two alternative attack the reaction between 3,5 diaminopyrazoles and N-ethoxy imidate . ΔE in kcal/mol

In Table 13 we have the activation energies associated to the transition states of the different steps in the mechanism for the synthesis of pyrazolo [1,5-a] [1,3,5] triazinones in gas phase and the established energetic diagram are shown in Fig. 9. In similar manner, the aminopyrazole R1 reacts with the N-ethoxy imidate under acidic condition to afford the corresponding intermediate I_1 . Cyclization of the resulted hydrazone followed by a deprotonation gave the desired pyrazolotriazinone. (Schema 4)

Table 13. Activation energies in (kcal/mol) for different step of the reaction between 3,5 diaminopyrazoles and N-ethoxy imidate to give P2 (a-b), in gas phase, calculated at the DFT/631++(d,p): gd3bj level (reference energy is the energy of the reactants)

TS	E_{a1}	E_{a2}	E_{a3}	E_{a4}
P2-a	21.6	33.7	37.0	15.7
P2-b	18.4	34.7	37.6	9.2

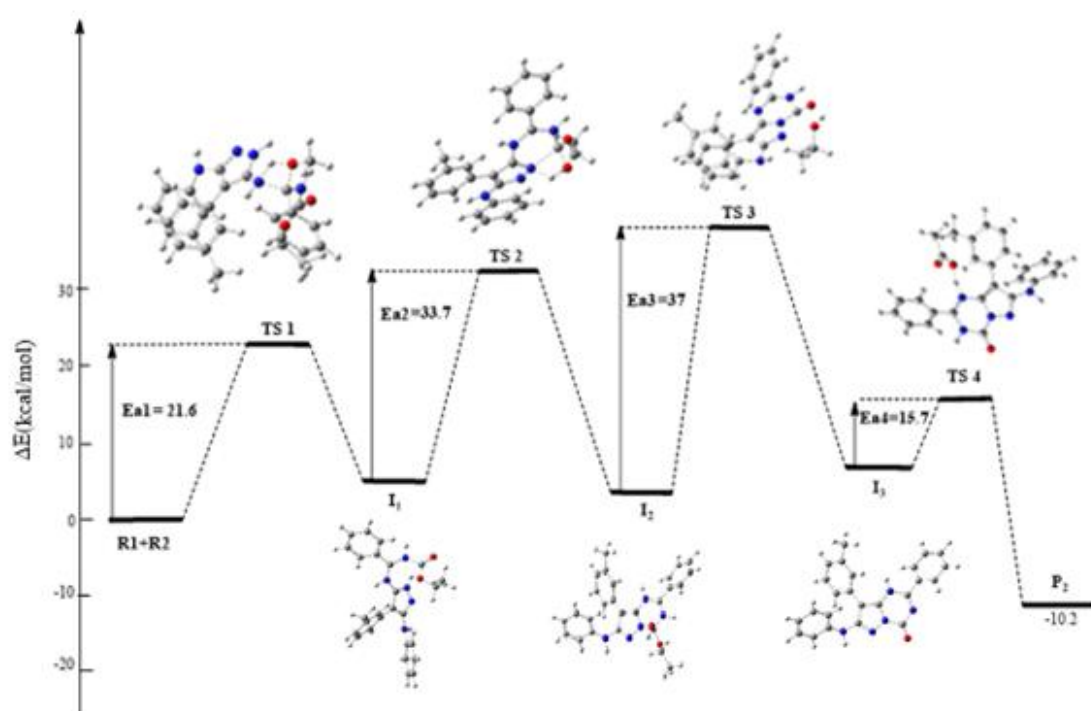
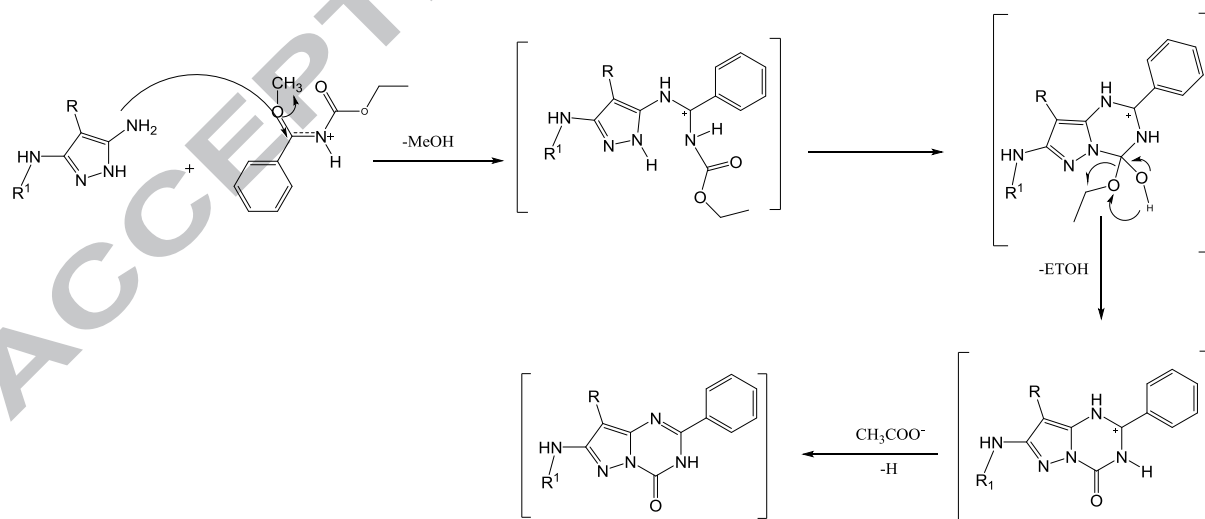


Fig. 9. Energy diagram of the reaction of 3,5-diaminopyrazoles with N-ethoxy imidate (P2a)

Scheme 4 Proposed mechanism for synthesis of pyrazolo [1,5-a] [1,3,5] triazinones



4 Conclusion

In conclusion, syntheses of a series of pyrazolo[1,5-a]-[1,3,5]-triazines or pyrazolo [1,5-a] [1,3,5] triazinones are described through DFT calculations at the B3LYP-D3(BJ)/6-31 ++G(d,p) level of theory. The reactivity of the series of diaminopyrazole with N-acyl imidates or the N-ethoxy imidate are studied using hardness, softness and global electrophilicity index as well as the FMO theory. It shows that obtaining pyrazolo[1,5-a]-[1,3,5]-triazines or

pyrazolo [1,5-a] [1,3,5] triazinones is only possible through a proton exchange between N-acyl imidates or the N-ethoxy imidate and (acetic) acid. After the protonation of R2 they become more reactive and the intervention of the acetic acid on R2 changes the site of attack to obtain the experimental product. The study of the local reactivity of diaminopyrazole with N-acyl imidates or the N-ethoxy using Fukui Function and natural charges proves that the reaction is under charge control and this reaction takes place along a mechanism in several steps. Finally, the proposed mechanism, which is based on nucleophilic substitution, leads to the obtained product, allowing experimentalists to a better understanding of the studied reaction.

Acknowledgements

The Grand Équipement National de Calcul Intensif/CINES for HPC resources/computer time is acknowledged for a grant of time (Project cpt2130).

Funding sources

This research did not receive any specific grant from funding agencies in the public, commercial, or not-for-profit sectors.

References

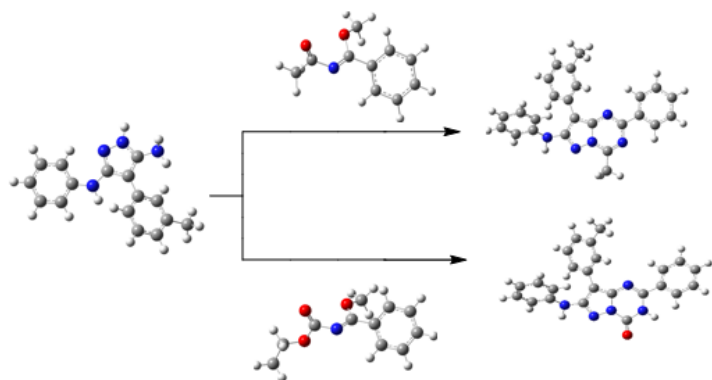
- [1] R. Dua, S. Shrivastava, S.K. Sonwane, and S. K. Srivastava, J. Advan. Biol. Res., 5 (2008) 120.
- [2] A. V. Dolzhenko, W. K. Chui, Heterocycles. 75 (2008) 1575–1622.
- [3] N.M. Abunada, H.M. Hassaneen, N.G. Kandile, O.A. Miqdad, Molecules. 13 (2008) 1501-1517.
- [4] A. El-Shafei, A.A. Fadda, A.M. Khalil, T.A.E. Ameen, F.A. Badria, Bioorg. Med. Chem. 17 (2009) 5096-5105
- [5] S.A.A. El Bialya, M.A. Gouda, J. Heterocycl. Chem. 48 (2011) 1280-1286
- [6] G. H. Elgemeie, S. R. El-Ezbawy, H. A. Ali, Synth. Commun., 31 (2001) 3459-3467.
- [7] S. Checchi and M. Ridi, Gazz. Chim. Ital., 87 (1957) 597-614.
- [8] G. H. Elgemeie, S. R. El-Ezbawy, H. A. El-Aziz, Synth. Commun., 31 (2001) 3453-3458.
- [9] M. L. Efrit, DEA, Fac. Sci. Tunis, Tunisie (1984).
- [10] M. T. Kaddachi, These de specialite, Fac. Sci. Tunis, Tunisie (1988).
- [11] K. Bokri, M.L. Efrit, A. B. Akacha, Heterocyclic Letters, 5 (2015) 679-685.
- [12] R.G. Pearson. J Am Chem Soc. 85 (1963) 3533–3539.
- [13] R.G. Pearson, Acids and bases. Science 151 (1966) 172–177.

- [14] R.G. Parr, R.G. Pearson, *J Am Chem Soc.* 105 (1983) 7512–7516
- [15] R.G. Pearson, *Chemical hardness: applications from molecules to solids*, Wiley-VCH, Oxford (1997).
- [16] R.G. Pearson, *Coord. Chem. Rev.* 100 (1997) 403–425
- [17] G. Salgado-Morán, S. Ruiz-Nieto, L. Gerli-Candia, N. Flores-Holguín, A. Favila-Pérez, D. Glossman-Mitnik. *J. Mol. Model.* 19 (2013) 3507
- [18] M.J. Frisch et al., *Gaussian 09, Revision A. 02*, Gaussian Inc., Wallingford, CT; 2009.
- [19] A.D. Becke, *J Chem Phys.* 98 (1993), 5648–5652
- [20] C. Lee, W. Yang, R.G. Parr, *Phys. Rev. B* 37 (1988) 785–789
- [21] S. Grimme, S. Ehrlich and L. Goerigk, *J. Comp. Chem.*, 32, 2011, 1456–1465.
- [22] H. Schröder, A. Creon, T. Schwabe, *J. Chem. Theory Comput.* 2015, 11, 7, 3163–3170
- [23] H.B. Schlegel, *J. Comput. Chem.* 3 (1982) 214.
- [24] A.D. McLean, G.S. Chandler, *J. Chem Phys* 72 (1980) 5639–5648
- [25] R. Krishnan, J.S. Binkley, R. Seeger, J.A. Pople, *J. Chem Phys* 72 (1980) 650–654
- [26] V. Barone, M. Cossi, *J. Phys. Chem. A*, 102 (1998) 1995
- [27] D. Li, H. Zhao, Z. Lin, *Organometallics*, 26 (2007) 2824–2832.
- [28] M.H. Gordon, J.A. Pople, *J. Chem. Phys.* 89, (1988), 5777.
- [29] T.A. Koopmans, *Physica* 1 (1933) 104.
- [30] A.E. Reed, L.A. Curtiss, F. Weinhold, *Chem. Rev.* 88 (1988) 899–926.
- [31] M.J. Frisch, G.W. Trucks, H.B. Schlegel, G.E. Scuseria, M.A. Robb, J.R. Cheeseman, G. Scalmani, V. Barone, B. Mennucci, G.A. Petersson, H. Nakatsuji, M. Caricato, X. Li, H.P. Hratchian, A.F. Izmaylov, J. Bloino, G. Zheng, J.L. Sonnenberg, M. Hada, M. Ehara, K. Toyota, R. Fukuda, J. Hasegawa, M. Ishida, T. Nakajima, Y. Honda, O. Kitao, H. Nakai, T. Vreven, J.A. Montgomery, J.E. Peralta, F. Ogliaro, M. Bearpark, J.J. Heyd, E. Brothers, K.N. Kudin, V.N. Staroverov, R. Kobayashi, J. Normand, K. Raghavachari, A. Rendell, J.C. Burant, S.S. Iyengar, J. Tomasi, M. Cossi, N. Rega, J.M. Millam, M. Klene, J.E. Knox, J.B. Cross, V. Bakken, C. Adamo, J. Jaramillo, R. Gomperts, R.E. Stratmann, O. Yazyev, A.J. Austin, R. Cammi, C. Pomelli, J.W. Ochterski, R.L. Martin, K. Morokuma, V.G. Zakrzewski, G.A. Voth, P. Salvador, J.J. Dannenberg, S. Dapprich, A.D. Daniels, O. Farkas, J.B. Foresman, J.V. Ortiz, J. Cioslowski, D.J. Fox, *Gaussian 09, Revision B.01*, Gaussian, Inc., Wallingford, CT, 2010.
- [32] H. Chermette, *J. Comp. Chem.* 20 (1999) 129–154
- [33] J. Padmanabhan, U. Sarkar, P.K. Chattaraj, R. Parthasarathi, V. Subramanian, *Chem. Phys. Lett.* 383 (2004) 122–128

- [34] P.K Chattaraj, R.G. Parr, K.D. Sen K, D.M.P. Mingos, in Chemical hardness, Structure and bonding, Springer: Berlin, 80 (1993) 11–25
- [35] P. Mondal, K. Hazarika, R. Deka, Phys. Chem. Commun. 6 (2003) 24–27.
- [36] P. Geerlings, F. De Proft, W. Langenaeker, Chem. Rev. 103 (2003) 1793–1873
- [37] R.G. Parr, W. Yang, J. Am. Chem. Soc. 106 (1984) 4049.
- [38] R.G. Parr, R.G. Pearson, J. Am. Chem. Soc. 105 (1983) 7512.
- [39] R.G. Parr, L. Von Szentpaly, S. Liu, J. Am. Chem. Soc. 121 (1999) 1922.
- [40] H. Chermette, P. Boulet, S. Portmann, in: K.D. Sen Fukui functions and local softness, reviews in modern quantum chemistry: a celebration of the contributions of Robert G. Parr, 2002; recent advances in density functional methods, part V, World Scientific, Singapore, (2002), 992–1012
- [41] W. Yang, W.J. Mortier, J. Am. Chem. Soc. 108 (1986) 5708–5711
- [42] A.E. Reed, L.A. Curtiss, F. Weinhold, Chem. Rev. 88 (1988) 899–926
- [43] C. Morell, A. Grand, A. Toro-Labbé. J. Phys. Chem. A. 109 (2005) 205–212
- [44] C. Morell, A. Grand, A. Toro-Labbé, Chem. Phys. Lett. 425 (2006) 342–346

Highlights

- Theoretical results allowed to explain the regioselectivity observed experimentally for synthesis of pyrazolo[1,5-a][1,3,5]triazine and pyrazolo[1,5-a][1,3,5] triazinones.
- Geometry optimization of all reactants was carried out using DFT methods.
- Determine transition states of the different steps encountered in this reaction.
- Propose reaction mechanism by theoretical calculations.

Graphical abstract

Declaration of interests

☐ The authors declare that they have no known competing financial interests or personal relationships that could have appeared to influence the work reported in this paper.

☐ The authors declare the following financial interests/personal relationships which may be considered as potential competing interests:

--